

Nature and symmetry of the order parameter of the noncentrosymmetric superconductor Li_2Pt_3B

Soumya P. Mukherjee and Tetsuya Takimoto

*Asia Pacific Center for Theoretical Physics,
Hogil Kim Memorial building 5th floor, POSTECH,
Hyoja-dong, Namgu, Pohang 790-784, Korea*

(Dated: August 28, 2018)

Abstract

The nature and symmetry of the superconducting gap function in the noncentrosymmetric superconductor (NCS) Li_2Pt_3B , even many years after its discovery, appears to be full of contradictions. In this letter based on the existing band structure calculations we find that owing to the considerable nesting near the Fermi surface and the enhanced d-character of the relevant bands that cross the Fermi level, the system gets somewhat strongly correlated. Considering the effect of the onsite Coulomb repulsion on the pairing potential perturbatively, we extract possible superconducting transition. The strong normal spin fluctuation gives rise to a singlet dominant gap function with accompanying sign change. Thus our theory predicts a s_{\pm} wave gap function with line nodes as the most promising candidate in the superconducting state.

PACS numbers: 74.20.Mn, 74.20.Rp, 74.70.-b, 74.90.+n

The occurrence of superconductivity in compounds without spatial inversion symmetry is one of the most active fields of research now a days. Inversion symmetry breaking leads to many new interesting effects in the superconducting state. The discovery of superconductivity in Li_2Pd_3B [1] and subsequently the experiments in the pseudo-binary complete solid solution $Li_2(Pd_{1-x}Pt_x)_3B$, $x = 0 \sim 1$ [2] attracted much attention. Many experimental as well as theoretical works reported since then. The end compounds Li_2Pd_3B ($x = 0$) and Li_2Pt_3B ($x = 1$) [3–8] were also studied intensively and compared. It is now established that the superconductivity in Li_2Pd_3B is phonon mediated s-wave type. The presence of Hebel-Slichter peak in the Nuclear spin-lattice relaxation rate measurement [3, 4], low temperature behavior of the specific heat [5, 6], penetration depth [8] etc. as well as NMR Knight shift data strongly support this conclusion. On the other hand, the nature and symmetry of the gap function of the compound Li_2Pt_3B is still debatable. Similar experiments performed on this compound [4, 6, 8] suggest the presence of line nodes in the superconducting state. The NMR Knight shift, often used to distinguish the spin state of superconductivity between singlet and triplet, is almost temperature independent even below T_c . This behavior is also interesting and deserve special attention.

In this letter, based on the existing band structure calculations [9, 10] we find that there exists considerable nesting between the Fermi surfaces and enhanced d-character of the relevant bands that cross the Fermi level. These two effects lead to a stronger electron correlation in Li_2Pt_3B than in Li_2Pd_3B [11]. By treating this correlation perturbatively we estimate the effect of spin fluctuations on the stability of superconducting state [12]. Owing to the large usual spin fluctuation the singlet gap function becomes much stronger than the triplet gap function. The singlet gap function belongs to A_1 representation with sign change between two branches of the Fermi surface. Thus our theory suggests a singlet dominant s_{\pm} wave gap function with line nodes as the most promising candidate for the superconducting state of Li_2Pt_3B . This prediction also explains most of the experiments. We also calculate the behavior of uniform spin susceptibility below T_c and comment on the apparent mismatch with the experiment.

The crystal structure of the compound Li_2Pt_3B is simple cubic (with point group O) and isostructural with the compound Li_2Pd_3B . The only difference between them is in the mass of the central Pt and Pd atoms. However this gives rise to some significant observable effects [9, 10]. For Pt compound there is an enhancement of d-character of the bands that

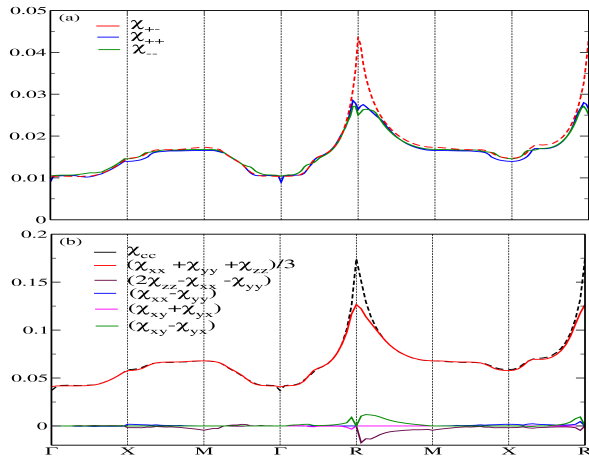


FIG. 1: (Color online) Signature of nesting.(a) Momentum dependence of interband and intraband susceptibilities showing nesting at $\mathbf{Q} = (\pi, \pi, \pi)$.(b)The comparison of the relative magnitudes of normal and anomalous spin fluctuations. The charge fluctuation χ_{cc} and normal spin fluctuation $\frac{1}{3}(\chi_{xx} + \chi_{yy} + \chi_{zz})$ contribute strongly compared to the anomalous spin fluctuations.The spin susceptibility also get enhanced at the R point (details in text).

cross the Fermi level. This enhancement of the d-character is reflected in the increased DOS at the Fermi level. Considering these, we can construct a minimal model Hamiltonian ($H = H_0 + H_1$) of Li_2Pt_3B which is given by the Hubbard model with an antisymmetric spin-orbit (SO) coupling term, where

$$H_0 = \sum_{\mathbf{k}\sigma\sigma'} ([\varepsilon_{\mathbf{k}} - \mu] \hat{\sigma}_o + \mathbf{g}_{\mathbf{k}} \cdot \hat{\sigma})_{\sigma\sigma'} c_{\mathbf{k}\sigma}^\dagger c_{\mathbf{k}\sigma'}, \quad (1)$$

and $H_1 = U \sum_i n_{i\uparrow} n_{i\downarrow}$. Here $c_{\mathbf{k}\sigma}$ and $c_{\mathbf{k}\sigma}^\dagger$ denotes the annihilation and creation operators of an electron with momentum \mathbf{k} and spin σ . $\varepsilon_{\mathbf{k}}$ is the dispersion of electrons and μ the chemical potential. $\mathbf{g}_{\mathbf{k}} = -\mathbf{g}_{-\mathbf{k}}$ denotes the effective anti-symmetric SO coupling which breaks the inversion symmetry. In H_1 , U is the screened on-site interaction. The dispersion of electrons $\varepsilon_{\mathbf{k}}$ is constructed by the tight-binding method including upto fourth-neighbor hopping in the three-dimensional simple cubic lattice.

$$\begin{aligned} \varepsilon_{\mathbf{k}} = & 2t_1(\cos(k_x) + \cos(k_y) + \cos(k_z)) + 4t_2(\cos(k_x)\cos(k_y) + \cos(k_y)\cos(k_z) \\ & + \cos(k_z)\cos(k_x)) + 8t_3\cos(k_x)\cos(k_y)\cos(k_z) + 2t_4(\cos(2k_x) + \cos(2k_y) + \cos(2k_z)) \end{aligned} \quad (2)$$

The SO coupling term appropriate for the point group is given as $\mathbf{g}_{\mathbf{k}} = g(\sin(k_x), \sin(k_y), \sin(k_z))$. The values of the parameters ($t_1, t_2, t_3, t_4, g, \mu$) are chosen to be

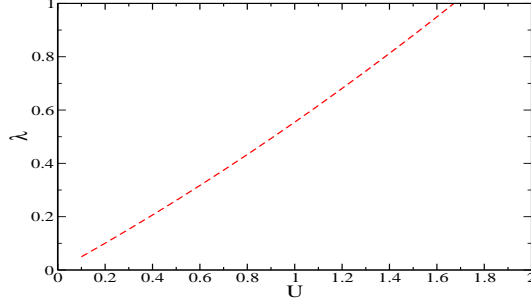


FIG. 2: (Color online) The variation of maximum eigenvalue with U .

(1.0, -0.03, -0.88, -0.03, 0.5, 0.02) as Fermi surface obtained by the band structure calculation are reproduced. One can diagonalize H_0 to get the eigen-energies $\varepsilon_{\mathbf{k}\pm} = \varepsilon_{\mathbf{k}} \pm |\mathbf{g}_{\mathbf{k}}| - \mu$. The spin degeneracy is now removed and $\varepsilon_{\mathbf{k}\pm}$ gives us the energy of the two helicity bands. The Fermi surfaces corresponding to the helically splitted bands consist of three major branches. One electron pocket around the Γ point, one hole pocket around the R point and other remaining parts forming a cage like structure with neck and mouth along $\Gamma - X$ direction. The corresponding parts of the Fermi surfaces of the different helicity bands are shifted from each other depending on the magnitude of g . Owing to the smallness of the parameters t_2, t_4 and μ there appears a large nesting with the nesting vector $\mathbf{Q} = (\pi, \pi, \pi)$ connecting between the cage like larger portion of the Fermi surface of the negative helicity band $\varepsilon_{\mathbf{k}-}$ and the similar cage like Fermi surface of the positive helicity band $\varepsilon_{\mathbf{k}+}$. Therefore this nesting gives rise to a sharp pick at the R point in the momentum dependence of $\chi_{+-}(\mathbf{q}) = \frac{1}{8N_0} \sum_{\mathbf{k}} \frac{f(\varepsilon_{\mathbf{k}-}) - f(\varepsilon_{\mathbf{k}+\mathbf{q}+})}{\varepsilon_{\mathbf{k}+\mathbf{q}+} - \varepsilon_{\mathbf{k}-}}$ where nesting condition is satisfied. There also exists partial nesting between Fermi surfaces around $\Gamma-$ and R-points of both helicity bands but for positive helicity band it's larger as shown in Fig. 1(a). The most general form of the matrix gap function is $\hat{\Delta}_{\mathbf{k}} = [\Psi(\mathbf{k})\hat{\sigma}_0 + \mathbf{d}(\mathbf{k})\cdot\hat{\sigma}]i\hat{\sigma}_y$. Here $\Psi(\mathbf{k})$ is the singlet gap function and $\mathbf{d}(\mathbf{k})$ is the triplet \mathbf{d} -vector. In NCS superconductor triplet component with $|\mathbf{d}(\mathbf{k})\cdot\mathbf{g}_{\mathbf{k}}| = |\mathbf{d}(\mathbf{k})||\mathbf{g}_{\mathbf{k}}|$ survive the pinning from the antisymmetric SO coupling [13]. So one can write $\mathbf{d}(\mathbf{k}) = \phi(\mathbf{k})\mathbf{g}_{\mathbf{k}}$ where $\phi(\mathbf{k})$ having the same symmetry of momentum dependence as $\Psi(\mathbf{k})$. With all these we can define the normal $\hat{G}(\mathbf{k}, i\omega_n)$ and anomalous $\hat{F}(\mathbf{k}, i\omega_n)$ matrix Green's functions as below,

$$\hat{G}(\mathbf{k}, i\omega_n) = G_+(\mathbf{k}, i\omega_n)\hat{\sigma}_0 + G_-(\mathbf{k}, i\omega_n)\tilde{\mathbf{g}}_{\mathbf{k}}\cdot\hat{\sigma}, \quad \hat{F}(\mathbf{k}, i\omega_n) = [F_+(\mathbf{k}, i\omega_n)\hat{\sigma}_0 + F_-(\mathbf{k}, i\omega_n)\tilde{\mathbf{g}}_{\mathbf{k}}\cdot\hat{\sigma}]i\hat{\sigma}_y \quad (3)$$

here $\tilde{\mathbf{g}}_{\mathbf{k}} = \mathbf{g}_{\mathbf{k}}/|\mathbf{g}_{\mathbf{k}}|$. G_{\pm} and F_{\pm} are given as,

$$G_{\pm}(\mathbf{k}, i\omega_n) = \frac{1}{2} \left(\frac{-i\omega_n - \varepsilon_{\mathbf{k}+}}{\omega_n^2 + E_{\mathbf{k}+}^2} \pm \frac{-i\omega_n - \varepsilon_{\mathbf{k}-}}{\omega_n^2 + E_{\mathbf{k}-}^2} \right), F_{\pm}(\mathbf{k}, i\omega_n) = \frac{1}{2} \left(\frac{\Delta_{\mathbf{k}+}}{\omega_n^2 + E_{\mathbf{k}+}^2} \pm \frac{\Delta_{\mathbf{k}-}}{\omega_n^2 + E_{\mathbf{k}-}^2} \right),$$

here $\Delta_{\mathbf{k}\pm} = \Psi(\mathbf{k}) \pm \phi(\mathbf{k})|\mathbf{g}_{\mathbf{k}}|$ and $E_{\mathbf{k}\pm} = \sqrt{\varepsilon_{\mathbf{k}\pm}^2 + \Delta_{\mathbf{k}\pm}^2}$. Within the weak coupling theory of superconductivity only static susceptibility is required. We start by defining the dynamical susceptibility as,

$$\chi_{\alpha\beta}(\mathbf{q}, i\Omega_n) = \int_0^{1/T} d\tau e^{i\Omega_n\tau} \langle T_{\tau} [S_{\mathbf{q}}^{\alpha}(\tau) S_{-\mathbf{q}}^{\beta}(0)] \rangle \quad (4)$$

here $\langle \dots \rangle$ denotes thermal average, T_{τ} imaginary time ordering and Ω_n are the Bosonic Matsubara frequencies. The charge (spin) operators with wave vector \mathbf{q} is defined as,

$$S_{\mathbf{q}}^c = \frac{1}{2} \sum_{\mathbf{k}\sigma} c_{\mathbf{k}\sigma}^{\dagger} c_{\mathbf{k}+\mathbf{q}\sigma}, \quad S_{\mathbf{q}}^{\alpha} = \frac{1}{2} \sum_{\mathbf{k}\sigma\sigma'} \sigma_{\sigma\sigma'}^{\alpha} c_{\mathbf{k}\sigma}^{\dagger} c_{\mathbf{k}+\mathbf{q}\sigma'} \quad (5)$$

With all these, the matrix elements of the static spin susceptibilities $\chi_{\alpha\beta}(\mathbf{q})$ for $\alpha, \beta = c, x, y, z$ is found to be,

$$\chi_{\alpha\beta}(\mathbf{q}) = \frac{1}{8N_0} \sum_{\mathbf{k}} \sum_{\xi\zeta} \Gamma_{\xi\zeta}^{\alpha\beta}(\mathbf{k}; \mathbf{q}) \frac{f(\varepsilon_{\mathbf{k}\xi}) - f(\varepsilon_{\mathbf{k}+\mathbf{q}\zeta})}{\varepsilon_{\mathbf{k}+\mathbf{q}\zeta} - \varepsilon_{\mathbf{k}\xi}}, \quad (6)$$

where $f(\varepsilon)$ is the Fermi distribution function and the function $\Gamma_{\xi\zeta}^{\alpha\beta}$ is obtained as,

$$\Gamma_{\xi\zeta}^{\alpha\beta}(\mathbf{k}; \mathbf{q}) = \delta_{\alpha,\beta}(1 - \xi\zeta\tilde{\mathbf{g}}_{\mathbf{k}} \cdot \tilde{\mathbf{g}}_{\mathbf{k}+\mathbf{q}}) + \xi\zeta(\tilde{g}_{\mathbf{k}\alpha}\tilde{g}_{\mathbf{k}+\mathbf{q}\beta} + \tilde{g}_{\mathbf{k}\beta}\tilde{g}_{\mathbf{k}+\mathbf{q}\alpha}) - \epsilon_{\alpha\beta\gamma}i(\xi\tilde{g}_{\mathbf{k}+\mathbf{q}\gamma} - \zeta\tilde{g}_{\mathbf{k}\gamma}). \quad (7)$$

Similarly the charge fluctuation in the normal state i.e. $\chi_{cc}(\mathbf{q})$ is obtained with the replacement of $\Gamma_{\xi\zeta}^{\alpha\beta}(\mathbf{k}; \mathbf{q})$ by $\Gamma_{\xi\zeta}^{cc}(\mathbf{k}; \mathbf{q})$ where $\Gamma_{\xi\zeta}^{cc}(\mathbf{k}; \mathbf{q}) = 1 + \xi\zeta\tilde{\mathbf{g}}_{\mathbf{k}} \cdot \tilde{\mathbf{g}}_{\mathbf{k}+\mathbf{q}}$. The susceptibilities between spin and charge operators $\chi_{c\alpha}(\mathbf{q})$ and $\chi_{\alpha c}(\mathbf{q})$ all vanishes for the static case. We calculate all the susceptibility components and examine the property of spin fluctuations. The usual spin fluctuation $\frac{1}{3}(\chi_{xx} + \chi_{yy} + \chi_{zz})$ with the momentum dependence of q^2 - type is also present in the centrosymmetric cubic system. Other symmetric spin fluctuations $(2\chi_{zz} - \chi_{xx} - \chi_{yy})$, $(\chi_{xx} - \chi_{yy})$ and $(\chi_{\alpha\beta} + \chi_{\beta\alpha})$ with $\alpha \neq \beta$ having momentum dependence $2q_z^2 - q_x^2 - q_y^2$, $q_x^2 - q_y^2$ and $q_{\alpha}q_{\beta}(\alpha \neq \beta)$ - types respectively are special to the cubic noncentrosymmetric case [12]. Along with these the anti-symmetric spin fluctuations $i(\chi_{\alpha\beta} - \chi_{\beta\alpha})$ with $\alpha \neq \beta$ with momentum dependence $q_{\gamma}(\gamma \neq \alpha \neq \beta)$ - type are also present. In Fig. 1(b) we compare relative strengths of the charge and usual spin fluctuation together with the anomalous spin fluctuations along symmetrical lines. Later we will see that the largeness of the usual spin fluctuation is responsible for the largeness of the singlet gap function as

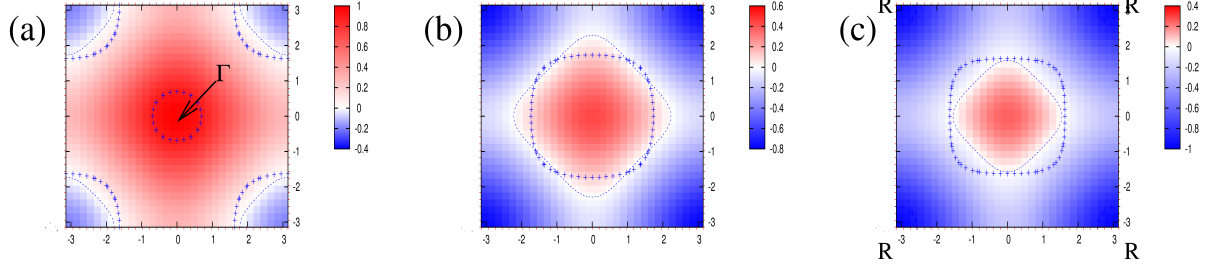


FIG. 3: (Color online) The singlet gap function at three k_z values; (a) $k_z = 0.0$, (b) $k_z = 0.7\pi$, and (c) $k_z = \pi$. Gap function varies from positive-maximum (Red) and to the negative-maximum (blue) following the scale attached with each figure. The blue line with + sign shows the Fermi surface of the positive helicity band while the dotted blue line denotes the nodes of the gap function (details in text).

triplet gap function whose magnitude is much smaller than the singlet one are induced by the antisymmetric spin fluctuations.

Treating the interaction term perturbatively and following the standard procedure [14–16] we arrive at the following superconducting gap equation,

$$\begin{pmatrix} \Psi(\mathbf{k}) \\ d_x(\mathbf{k}) \\ d_y(\mathbf{k}) \\ d_z(\mathbf{k}) \end{pmatrix} = \frac{1}{N_0} \sum_{\mathbf{q}} \begin{pmatrix} V_{ss}(\mathbf{q}) & V_{sx}(\mathbf{q}) & V_{sy}(\mathbf{q}) & V_{sz}(\mathbf{q}) \\ V_{xs}(\mathbf{q}) & V_{xx}(\mathbf{q}) & V_{xy}(\mathbf{q}) & V_{xz}(\mathbf{q}) \\ V_{ys}(\mathbf{q}) & V_{yx}(\mathbf{q}) & V_{yy}(\mathbf{q}) & V_{yz}(\mathbf{q}) \\ V_{zs}(\mathbf{q}) & V_{zx}(\mathbf{q}) & V_{zy}(\mathbf{q}) & V_{zz}(\mathbf{q}) \end{pmatrix} \begin{pmatrix} \mathcal{F}_s(\mathbf{k}-\mathbf{q}) \\ \mathcal{F}_x(\mathbf{k}-\mathbf{q}) \\ \mathcal{F}_y(\mathbf{k}-\mathbf{q}) \\ \mathcal{F}_z(\mathbf{k}-\mathbf{q}) \end{pmatrix}, \quad (8)$$

here $V_{\zeta\eta}$ with $(\zeta, \eta) = (s, x, y, z)$ denotes the pairing potential arising from the corresponding fluctuation exchange and they are expressed as below,

$$\begin{aligned} V_{ss}(\mathbf{q}) &= -U - U^2 [\chi_{xx}(\mathbf{q}) + \chi_{yy}(\mathbf{q}) + \chi_{zz}(\mathbf{q}) - \chi_{cc}(\mathbf{q})] \\ V_{\zeta\zeta}(\mathbf{q}) &= U^2 [\chi_{cc}(\mathbf{q}) + \chi_{\eta\eta}(\mathbf{q}) + \chi_{\delta\delta}(\mathbf{q}) - \chi_{\zeta\zeta}(\mathbf{q})] \\ V_{\zeta\eta}(\mathbf{q}) &= V_{\eta\zeta}(\mathbf{q}) = -U^2 [\chi_{\zeta\eta}(\mathbf{q}) + \chi_{\eta\zeta}(\mathbf{q})] \\ V_{s\zeta}(\mathbf{q}) &= -V_{\zeta s}(\mathbf{q}) = iU^2 [\chi_{\eta\delta}(\mathbf{q}) - \chi_{\delta\eta}(\mathbf{q})], \end{aligned} \quad (9)$$

where $\zeta \neq \eta \neq \delta$. Here \mathcal{F}_s and \mathcal{F}_α are the contributions from the anomalous Green's functions after frequency summation [14]. As we mentioned above the singlet component of the gap function arising from usual spin fluctuation dominates over triplet gap function which is induced by the small antisymmetric spin fluctuations. Eq. (8) reduces to the eigenvalue

problem if we work at the transition temperature T_c . We fix T_c arbitrarily at $0.02t_1$ and solve Eq. (8) for maximum eigenvalue. Fig. 2 gives us the critical value of the onsite interaction U for superconductivity i.e. $U_c = 1.675t_1$, when maximum eigenvalue becomes unity. We thus get the momentum dependence of both singlet and triplet gap functions as the eigenfunctions of the maximum eigenvalue. From the momentum dependence of the gap function we conclude that the superconductivity belongs to the A_1 representation of the point group O.

In Fig. 3 we present the contour plot of the singlet gap function at three k_z values in the 1st Brillouin zone. The singlet gap function changes sign from positive (red) to negative (blue) gradually moving from $\Gamma-$ to R-point and vanishes completely somewhere in between forming the nodal surface. Here we would like to mention that the gap function is strongest at either $\Gamma-$ or R-points although the nesting is rather weak here. On the other hand the cage like portion of the Fermi surface where we have most strongest nesting gives rise to weak gap function. It can be understood from a careful observation of Eq. (9). The summation of prefactor $\Gamma_{+-}^{\alpha\alpha}(\mathbf{k}, \mathbf{Q})$ of susceptibility $\chi_{\alpha\alpha}(\mathbf{Q})$ vanishes for the spin-singlet pairing potential $V_{ss}(\mathbf{Q})$ at the nesting vector $\mathbf{Q} = (\pi, \pi, \pi)$. Because of this, even strong interband nesting does not play any role in opening up the gap function. However, the pairing potential forms the gap on the Fermi surfaces around $\Gamma-$ and R-points, connected by sub-dominant nesting of $\chi_{++}(\mathbf{Q})$. Thus the singlet gap function with opposite signs between these points opens up and line nodes can exist in between. In this figure we show the corresponding zeros of the positive helicity Fermi surface by the + sign line and the dotted line denotes the exact location where the gap function vanish. In Fig. 3(a) around $\Gamma-$ point the gap is positive maximum. In Fig. 3(b) the strength of the negative gap function increases and finally, in Fig. 3(c) we encounter the maximum negative value of the gap function at the corner R-point. Thus the gap function appears to be singlet s_{\pm} type with accidental line nodes which is not allowed by symmetry, rather depend on the three-dimensional geometry of the Fermi surface.

We also calculate the temperature dependence of the susceptibility in the superconducting state. Within the weak coupling approximation neglecting the feedback effect we assume that the order parameter below T_c follows the BCS temperature dependence $\hat{\Delta}(\mathbf{k}, T) = \hat{\Delta}(\mathbf{k}, 0) \tanh(1.74\sqrt{\frac{T_c}{T}} - 1)$ at every momentum point. Using this gap function we calculate

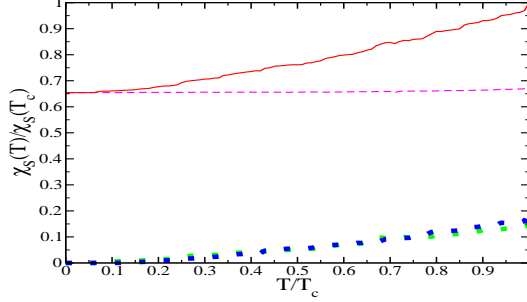


FIG. 4: (Color online) The variation of normalized spin susceptibility (solid red line) with temperature in the superconducting state. Also shown in the same figure the contributions from the Van-Vleck term (dashed magenta line) and the Pauli term of positive helicity band (green square) and negative helicity band (blue square), all scaled by $\chi_s(T_c)$.

the uniform susceptibility below T_c as follows [17].

$$\chi_s(T) = \sum_{\mathbf{k}} [\chi_0(\mathbf{k}, T) + \chi_+(\mathbf{k}, T) + \chi_-(\mathbf{k}, T)], \quad (10)$$

where $\chi_0(\mathbf{k}, T)$, $\chi_+(\mathbf{k}, T)$ and $\chi_-(\mathbf{k}, T)$ are given as,

$$\chi_0(\mathbf{k}, T) = \frac{1}{3} \sum_{\xi=\pm} \left[\left(1 - \xi \frac{\Delta_{\mathbf{k}+} \Delta_{\mathbf{k}-} + \epsilon_{\mathbf{k}+} \epsilon_{\mathbf{k}-}}{E_{\mathbf{k}+} E_{\mathbf{k}-}} \right) \times \left(\frac{\tanh(\frac{E_{\mathbf{k}+}}{2T}) + \xi \tanh(\frac{E_{\mathbf{k}-}}{2T})}{E_{\mathbf{k}+} + \xi E_{\mathbf{k}-}} \right) \right], \quad (11)$$

$$\chi_{\pm}(\mathbf{k}, T) = 1/(12T \cosh^2(E_{\mathbf{k}\pm}/2T)), \quad (12)$$

We plot in Fig. 4 the contribution from the temperature independent Van-Vleck term $\chi_0(T)$, temperature dependent Pauli terms $\chi_+(T)$, $\chi_-(T)$ and the susceptibility $\chi_s(T)$ all normalized by $\chi_s(T_c)$ (red line). Although $\chi_s(T)/\chi_s(T_c)$ shows excellent agreement with earlier works [18] but apparently contradicts the NMR Knight shift data [4]. To explain the contradiction with the experiment, one can formulate a multi-orbital theory which captures the complicated band structure in more detail. Then the large contributions of the Van-Vleck term between t_{2g-} and e_g- orbitals for cubic system is expected and this will further reduce the deviation of the normalized susceptibility from normal state below T_c . This involves somewhat elaborate calculations and we leave this as a future problem.

In conclusion, we suggest that, in the noncentrosymmetric superconductor Li_2Pt_3B considerable d-character of the bands near the Fermi energy and nesting of the Fermi surfaces give rise to weak correlation effect which can be treated perturbatively and this give rise to a singlet dominated (with negligible triplet component) s_{\pm} kind of gap function with accidental line nodes arising from the Fermi surface geometry. The three-dimensional geometry of

the Fermi surface and the nesting of the Fermi surface also play a crucial role in determining the nature of the gap function. We propose that angle-resolved photo emission spectroscopy and de Hass-van Alphen effect experiments may shed light on this nesting property of the Fermi surface and can be useful to study the properties of the superconducting state as well. We also calculate the susceptibility below T_c and emphasize the importance of orbital degeneracy of d-electron to explain the experimental data.

The authors are grateful to Y. Yanase for fruitful stimulating discussions during his visit in APCTP.

-
- [1] K. Togano, P. Badica, Y. Nakamori, S. Orimo, H. Takeya, and K. Hirata, Phys. Rev. Lett. **93**, 247004 (2004).
 - [2] P.Badica, T.Kondo, and K.Togano, J. Phys. Soc. Jpn. 74,1014 (2005).
 - [3] M. Nishiyama, Y. Inada, and G-Q Zheng, Phys. Rev. B **71**, 220505(R) (2005).
 - [4] M. Nishiyama, Y. Inada, and G-Q Zheng, Phys. Rev. Lett. 98, 047002 (2007).
 - [5] H. Takeya et. al., Phys. Rev. B **72**, 104506 (2005).
 - [6] H. Takeya, M. El Massalami, S. Kasahara, and K. Hirata, Phys. Rev. B **76**, 104506 (2007).
 - [7] P. S. Häfliger et. al., J. Supercond. Nov. Magn. 22, 337-342 (2009).
 - [8] H. Q. Yuan et. al., Phys. Rev. Lett. **97**, 017006 (2005)
 - [9] S. Chandra, S. Mathi Jaya, and M. C. Valsakunmar, Physics C **432**, 116 (2005).
 - [10] K. -W. Lee and W. E. Pickett, Phys. Rev. B **72**, 174505 (2005).
 - [11] T. Yokoya, T. Muro, I. Hase, H. Takeya, K. Hirata, and K. Togano, Phys. Rev. B **71**, 092507 (2005).
 - [12] T. Takimoto, J. Phys. Soc. Jpn.**77**, 113706 (2008).
 - [13] P. A. Frigeri, D. F. Agterberg, A. Koga, and M. Sigrist, Phys. Rev. Lett. **92**, 097001 (2004).
 - [14] T. Takimoto, and P. Thalmeier, J. Phys. Soc. Jpn.**78**, 103703 (2009).
 - [15] Y. Tada, N. Kawakami, S. Fujimoto, J. Phys. Soc. Jpn. 77, 054707 (2008).
 - [16] Y. Yanase and M. Sigrist, J. Phys. Soc. Jpn.**77**, 124711 (2008).
 - [17] P. A. Frigeri, D. F. Agteberg, and M. Sigrist, New Journal of Physics **6**, 115 (2004).
 - [18] K. V. Samokhin, Phys. Rev. B **76**, 094516 (2007).